Retrofitted Hybrid Power System Design With Renewable Energy Sources for Buildings

Y. Jaganmohan Reddy, Y. V. Pavan Kumar, K. Padma Raju, and Anilkumar Ramsesh

***Abstract*—Most of the research on Hybrid Power Systems (HPS) is to provide an economical and sustainable power to the rural electrification. This paper focuses on the design of an HPS for the building which is a part of the urban electrification. In the developing countries, the rate of increase in the demand is more than the rate of increase in the supply, which is a major challenge resulting in very frequent outages. There are number of motives to build integrated and synergistic renewable energy based HPS including environmental, economic, and social benefits. Most of these HPS topologies use inverters to interface the renewable sources to the buildings with an offering of low quality power. Hence, modern sustainability initiatives call for a design for both new HPS and retrofitting of an existing HPS topology. With this aspect, this paper describes the topology of retrofitting HPS with dc Motor-Synchronous Generator set instead of the use of inverter to an existing building power system. This can improve the power quality, reliability of the supply, and ensures stable plant operation. The proposed HPS topology can be used in small-to-medium sized isolated constructions like green buildings, industries, and universities. Different renewable energy sources like Photo Voltaics (PV), Wind Power (WP), and Fuel Cells (FC) are integrated to form HPS. An energy management and control algorithm is proposed to use the energy sources optimally to upgrade these buildings with more reliability and efficiency. The modeling and simulation is done using MATLAB/Simulink.**

***Index Terms*—DC Motor-Synchronous generator (MG) set, energy management and control unit (EMCU), Hybrid Power System (HPS), inverter, island and grid connected operations, power quality.**

I. Introduction

ELECTRICAL energy is essential to everyone's life no matter for whom or where they are. This is especially true in this new century, where people aim to pursue a higher quality of life. It is now a globally accepted reality that electrical energy is fundamental for social and economic development. Unfortunately, still one third of the world's population lives in developing and threshold countries and has no access to electricity [24]. It has been estimated that the world population will reach eight billion by 2020. And this growth is mostly in developing countries [25]. So, to supply the electricity requirements for them, the extension of utility grid is complicated and expensive due to geographical and economical barriers. Besides, the need for unrelenting increment in energy production, diminution in currently reliant fossil fuel resources, and the regulations to reduce the $\mathrm{CO_2}$ emissions is the foremost factor for stipulating the growth of "green energy" generation systems. In such circumstances, an alternative is to use locally available renewable energy sources (e.g., solar, wind, hydrogen, and etc.) and combine to implement modular, expandable, and task-oriented systems known as the HPS. HPS combine two or more energy conversion devices, or two or more fuels for the same device, that when integrated, overcome the limitations inherent in either.

Multi-source HPS with proper control has a higher potential for providing better quality and more reliable power to utilities than a system based on a single resource. These are generally independent of the large centralized utility grid. Generally, HPS use a combination of conventional non renewable energy sources like fossil fuel, hydal energy, nuclear energy, or a combination of renewable energy sources like solar energy, wind energy, etc., and may be a combination of both renewable and non renewable energy sources. The HPS discussed in this paper is a combination of only renewable energy sources like solar cells, fuel cells, and wind energy systems. This is clean and abundantly available in nature. It offers many advantages over conventional fossil fuel based power generation systems, such as low pollution, high efficiency, diversity of fuels, and on-site installation.

Keeping all these in mind, many decentralized HPS have been installed worldwide. One of the major applications of the proposed HPS is to meet the power supply needs of a "green building." On the aesthetic side of green architecture or sustainable design is the philosophy of designing a building that is in harmony with the natural features and resources surrounding the site. These buildings are aimed for optimum usage of energy resources by reducing waste of energy and toxics, pollution free generation, durability, and comfort [8], [26]–[28].

II. Prior Art and Problem Identification

In general, all HPS architectures can be grouped into island mode and grid connected mode layouts [30]–[32]. All these might contain ac diesel generators [11], diesel system, an ac or dc distribution system, loads, energy sources, energy storage, power converters, load management options or a supervisory [20], etc.

These two HPS classifications are as follows:

- Stand-alone/off-grid/Islanding—HPS, which are independent of the utility grid, used to meet the load demands especially at remote places; and
- Grid connected HPS, which are connected in parallel with the central utility power grid and can be used at any location (rural or urban).

Manuscript received November 27, 2011; revised April 29, 2012; accepted August 28, 2012. Date of publication December 10, 2012; date of current version December 28, 2012. Paper no. TSG-00622-2011.

Y. J. Reddy, Y. V. P. Kumar, and A. Ramesh are with the Honeywell Technology Solutions Lab (Pvt) Ltd, Hyderabad, Andhra Pradesh, India (e-mail: jaganmohan.reddy@honeywell.com; yvpavan.kumar@honeywell.com; anilkumar.ramsesh@honeywell.com).

K. P. Raju is with the Department of Electronics and Communication Engineering, Jawaharlal Nehru Technological University Kakinada, Andhra Pradesh, India (e-mail: padmaraju_k@yahoo.com).

Color versions of one or more of the figures in this paper are available online at http://ieeexplore.ieee.org.

Digital Object Identifier 10.1109/TSG.2012.2217512

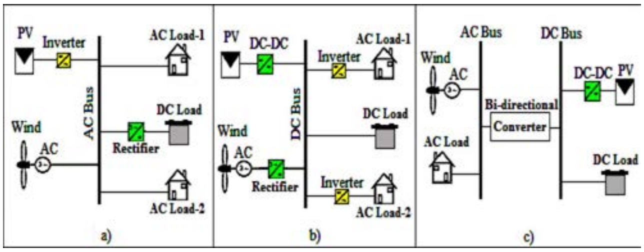

Fig. 1. Different architectures of standalone HPS.

A. Stand Alone/off Grid/islanding HPS

Stand alone HPS are designed and sized to attend specific loads. The power units commonly used are PV panels (dc source), WP and Diesel Generators (ac sources). Batteries are often used for storage and backup. Other power electronics components like rectifiers, inverters, and/or converters are used to match the ac and dc generation source with the voltage and frequency requirements of the load. The control system for HPS configurations should minimize fuel consumption by maximizing power from the renewable sources [29]. There are power fluctuations by the variability of the renewable energy, which cause disturbances that can affect the quality of the power delivered to the load. Fig. 1 shows the basic architectures of standalone HPS.

In centralized ac-bus layout shown in Fig. 1(a), all the energy sources and the loads are connected to an ac bus. DC sources are needed to have the inverters to convert dc to ac before connecting to ac bus. It is more modular configuration, which facilitates the growth to manage the increasing energy needs. It offers major constraint in the synchronization of the inverters and ac sources to maintain the voltage and frequency of the system. The undesired harmonics introduced into the system by the use of inverters increases the level of power quality problems.

In centralized dc-bus layout shown in Fig. 1(b), all the energy sources and the loads are connected to a dc bus. All the ac sources needed to have the rectifiers to convert ac to dc before connecting to dc bus. DC loads can be connected directly to the dc bus, which reduces the harmonic pollution from power electronic equipment. The dc bus eliminates the need for frequency and voltage controls of the generation source connected to the bus. This design has a limitation in efficiency because of passing through two stage conversion between source and load in the case where both source and load are operating on ac.

The ac/dc-bus layout shown in Fig. 1(c) has both ac and dc buses. The ac sources and loads are directly connected to ac bus. Similarly, the dc sources and loads are connected to dc bus. Both buses are connected through a bidirectional converter that permits power flow between the two buses. This arrangement increases the system power reliability and supply continuity.

B. Grid Connected HPS

Different grid connected architectures [5], [16], [25] are shown in Fig. 2. Each system has its own advantages and disadvantages. The choice of the layout for particular location depends upon geographical, economical and technical factors.

In centralized ac-bus architecture shown in Fig. 2(a), the sources and the battery are all installed in one place and are connected to a main ac bus bar before being connected to the grid. This system is centralized in the sense that the power delivered by all the energy conversion systems and the battery is fed to the grid through a single point. In this case, the power

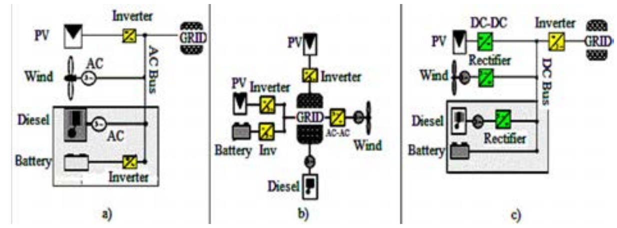

Fig. 2. Different architectures of grid connected HPS.

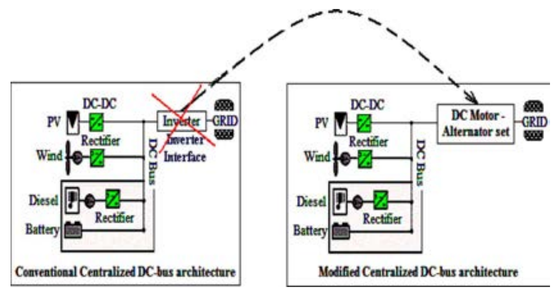

Fig. 3. Comparison of conventional and retrofitted HPS.

produced by the PV system and the battery is inverted into ac before being connected to the ac bus.

In distributed ac-bus architecture shown in Fig. 2(b), the power sources do not need to be installed close to each other, and they do not need to be connected to one main bus. The sources are distributed in different geographical locations and connected to the grid separately. The power produced by each source is conditioned separately to be identical with the form required by the grid. The main drawback of this architecture is the difficulty of controlling the system when the diesel generator is in off mode.

The centralized dc-bus architecture shown in Fig. 2(c) utilizes a main centralized dc bus bar. So, the energy conversion systems that produce ac power, namely the WP and the diesel generator, firstly deliver their power to rectifiers to be converted into dc before being delivered to the main dc bus bar. A main inverter takes the responsibility of feeding the ac grid from this dc bus.

C. Cumulative Merits/Demerits of HPS Architectures

The existing HPS architectures have the following constraints as identified from the study in Sections II-A and II-B.

Island mode:

- Centralized ac-bus layout has a more modular configuration, facilitating growth to manage increasing energy needs. It comes with major constraints in the synchronization of the inverters and ac sources to maintain the voltage and frequency of the system. The undesired harmonics introduced into the system by the use of inverters increases the level of power quality problems.
- Centralized dc-bus layout reduces the harmonic pollution from power electronic equipment. The dc bus eliminates the need for frequency and voltage controls of the generation source connected to the bus. This design offers an advantage in the fuel consumption, which is 10% to 14% lower compared to the other architectures but with a limitation in efficiency because of passing through a two stage conversion between source and load in the case where both source and load are operating on ac.
- The ac/dc-bus layouts increase the system power reliability and supply continuity, and are associated with the merits and demerits of both centralized ac and dc architectures.

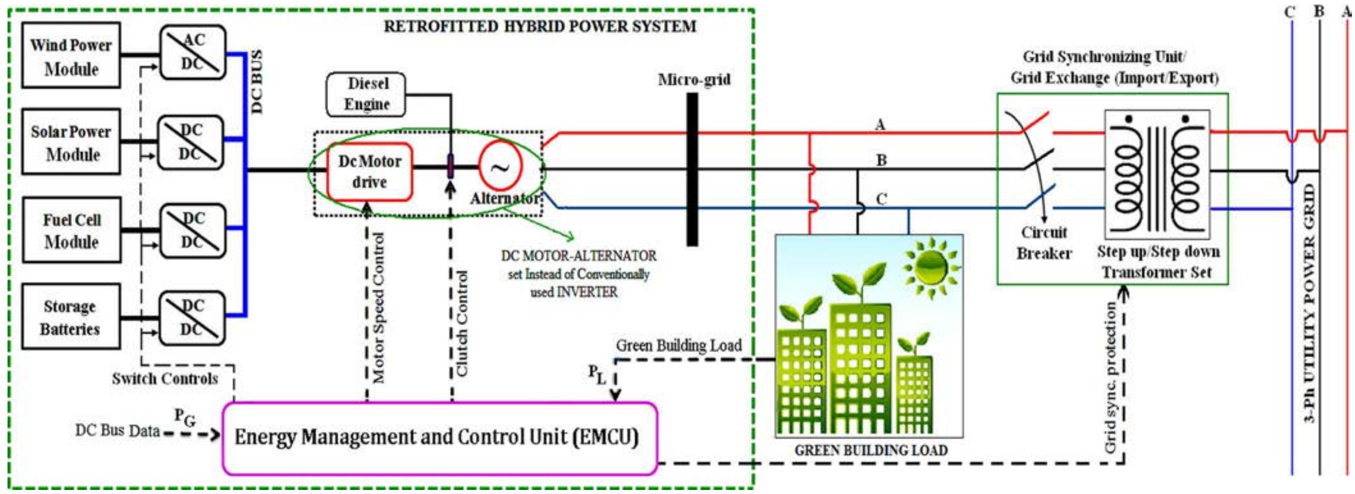

Fig. 4. The architecture of the retrofitted HPS connected to the building and running in parallel with utility grid.

Grid connected mode:

- In general, most of the renewable energy resources operate on dc. Hence, in a centralized ac-bus architecture all the dc sources require as many inverters to connect them to the ac bus. This leads to system power quality issues.
- The main drawback of distributed ac-bus architecture is the difficulty in controlling the system when the diesel generator is in off mode.
- The centralized dc bus architecture eliminates the requirement for more inverters, leading to a chance of improving power quality.

"Cumulatively, these architectures lag in terms of power quality, which limits the system to connect to the central utility grid. Also, they lack in effective energy management between energy sources and loads to increase the utilization, reliability, and stability of the supply."

The proposed retrofitted HPS architecture can overcome most of these limitations and facilitate grid-connected mode of operation to improve the supply reliability to buildings.

III. Retrofitted Hybrid Power System Architecture for Buildings

The HPS investigated and retrofitted in this paper consists of renewable energy sources such as PV, FC, WP, and also storage batteries. Most of these (PV, FC, and Batteries) are producing dc output. Hence, the centralized dc-bus architecture for grid connected HPS shown in Fig. 2(c) has been chosen in this paper.

A. Methodology Used in the Design

The methodology that is implemented in this paper uses dc Motor-Synchronous generator set instead of Inverter between the dc bus and the loads/microgrid in the conventional HPS for buildings. That is, exactly in between the dc bus and the building loads/grid as shown in the following Fig. 3.

Also, the proposed EMCU takes the power demand and the power generated at any instant as inputs. Based on these two factors, it can switch the available resources to meet the instantaneous connected load. This reduces the wastage of energy, and hence unit generation cost, also provides the facility to run the building power generating system in parallel with the utility power grid.

B. Proposed System Description

In the system shown in Fig. 4, the output of the renewable sources cannot feed the load directly, as the voltage fluctuations due to environmental variations are large enough to damage the concerned load [14].

The (dc-dc)/(ac-dc) converters are used to condition these voltages. Thus, the varying voltage can be brought to required value and specified variations limits by varying the duty ratio of the converters, and then connected to dc bus. The dc bus voltage is used to drive the dc motor, coupled to the synchronous generator. Electrical power should be produced exactly at the same time when it is demanded by building load. It may not be possible for renewable energy sources to produce sufficient energy to drive dc motor coupled to synchronous generator at all the time, since their operation depends on varying natural conditions. The WT output power varies with the wind speed, the PV cell output power varies with both the temperature and irradiance, and the FC output power varies with input fuel. So, the diesel engine is coupled to synchronous generator as a standby prime mover to avoid shortages of power. The dc motor, Alternator and Diesel Engine are mechanically connected using a clutch.

The dc bus integrates all the energy sources and storage batteries. To have an optimum, efficient, and reliable operation of the complex system consist of various power sources, a control is needed [23]. Hence microgrid controller called as Energy Management and Control Unit (EMCU) is designed using the algorithm proposed in Fig. 14. The MATLAB/Simulink [2] model for the retrofitted HPS is shown in Fig. 13. This EMCU manages/operates the available resources with respect to the load requirement and also provides facility for grid interaction to export/import the power with respect to deficit and excess power conditions. This increases stability and reliability of the system.

In the system shown in Fig. 4, the grid synchronizing unit takes input from EMCU and provides the operation of grid export/import through circuit breaker and transformer based on the condition of load demand and the generated power. This will also isolate the system from grid under emergency situations like faults, which leads to loss of synchronism. Whenever the HPS is unable to meet the load demand, then the grid will feed the load and similarly, whenever excess energy is there from the HPS, it will feed the grid. This could be possible because of

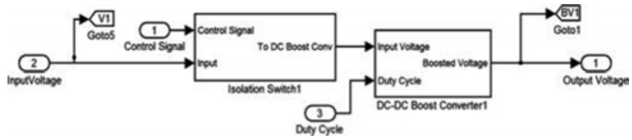

Fig. 5. MATLAB/Simulink model of Local Controller.

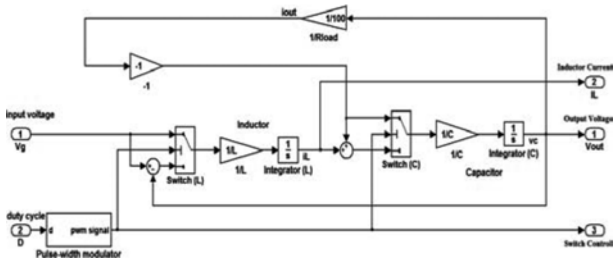

Fig. 6. MATLAB/Simulink model of a boost converter.

the improvement in power quality with the proposed retrofitted HPS architecture with EMCU.

IV. Modeling and Simulation

All the constituents of the retrofitted HPS shown in Fig. 4 such as PV cells [10], [14], Fuel cells [1], [3] and its Electrolyzer [5], [6], Wind power [7], [9], [21], [22], and batteries [36], [37] are modeled in MATLAB/Simulink, based on the mathematical equations given in [14], [33]–[35], and the other models specific to the proposed system are given as follows.

A. Local Controller/DC-DC Boost Converter

The local controllers are acting in between the energy resources and the dc bus as shown in Fig. 13. The local controller takes the control signal from EMCU and switches the energy resources accordingly. This is based on the conditions of load and environment. The local controller consists of an isolation switch for the purpose of isolating particular resource from dc bus as per EMCU signal, and dc-dc boost converter arrangement to boost up the voltage so as to meet dc bus voltage as shown in Fig. 5.

Fig. 6 shows the MATLAB/Simulink model of the dc-dc boost converter with the state equations [6] and the values [38] as follows. The typical parameters to be entered are given in Table I.

$$\frac{di_L}{dt} = \frac{-r_L}{L} \cdot i_L - \frac{(1-k)}{L} \cdot V_C + \frac{1}{L} \cdot u(t) \tag{1}$$

$$\frac{dV_C}{dt} = \frac{(1-k)}{C} \cdot i_L - \frac{1}{C \cdot R_L} . V_C \tag{2}$$

The dc-dc boost converter step up the dc voltage to the desired value by varying its duty cycle as a ratio of voltages (δ), and is given by (3)

$$\delta = \frac{V_{out} - V_{in}}{V_{out}} \tag{3}$$

where;

V_{out} desired output voltage;

V_{in} input voltage.

TABLE I
Typical Parameters Involved in Boost Converter Modeling

S. No	Parameter	Values
1.	Inductance L (μH)	250
2.	Output capacitance C (μF)	50
3.	Inductance series resistance r_L (Ω)	0.1
4.	Capacitance series resistance r_C (Ω)	0.1
5.	Load resistance R_L (Ω)	25
6.	Input voltage U(t) in Volts	100
7.	Reference o/p voltage V_{ref} (Volts)	230
8.	Switching frequency F_s (kHz)	50

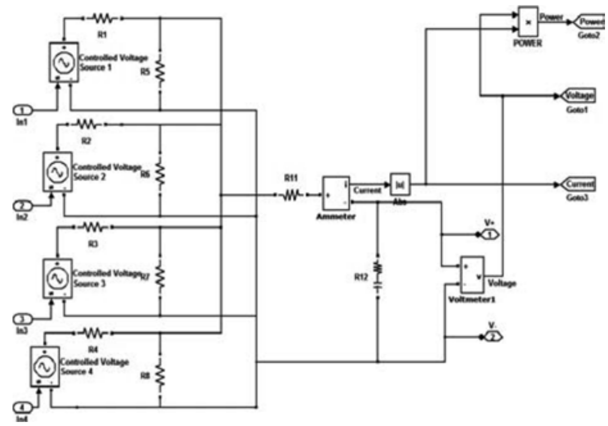

Fig. 7. MATLAB/Simulink model of the dc bus.

B. DC Bus Connections

The dc bus is the parallel interconnection of all the resources. The output of energy resources is initially given to local controller and from then it is given to the dc bus to form a centralized dc bus architecture. Fig. 7 shows the MATLAB/Simulink model of the dc bus. From this, the dc Power is fed to the further parts of the system. The next section to the dc bus is Inverter/dc Motor-Alternator system which is operated based on the inputs from dc bus.

C. Modeling of the Inverter Circuit

Inverter is an electronic circuit for converting input dc voltages to output three phase ac voltages. For the HPS conventional design it is needed to design a three phase inverter circuit. Generally it is designed with power electronic components like Diodes, IGBT, or Thyristors. Fig. 8 shows the power electronic IGBT/Diodes based inverter circuit and the typical parameters to be entered are given in Table II.

Fig. 9 shows the circuit of giving firing angles for controlling the operation of inverter arms. This circuit have PID (Proportional, Integral, and Derivative) controller to provide necessary control action with respect to the output voltage of the inverter. The input for the PID controller is a difference signal of the feedback signal of inverter output and the reference voltage signal.

D. DC Motor/Diesel Engine-Synchronous Generator Set

In order to improve power quality, the dc bus voltage is used to drive motor-synchronous generator set instead of inverter [15], [16] as the Matlab/Simulink model shown in Fig. 10. The speed control circuit [22] is shown in Fig. 11. For dc Motor model, select Four-Quadrant Chopper dc Drive in Sim power systems/machines from simulink library browser with the set point of speed 1500 rpm, field voltage of 230 Volts, and in

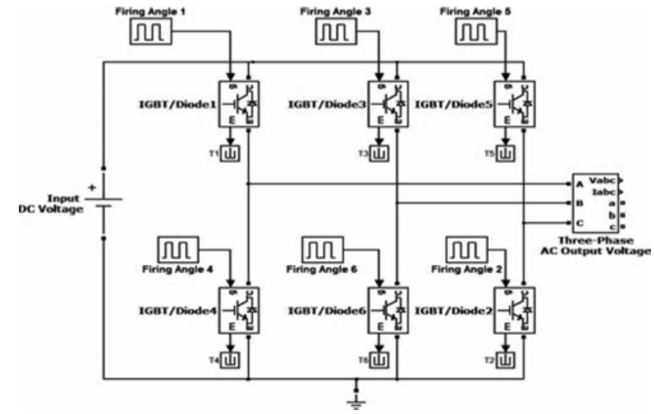

Fig. 8. MATLAB/Simulink model of Inverter.

TABLE II
PARAMETERS USED IN INVERTER MODELING

S. No	Parameter	Description
1.	Number of bridge arms	3
2.	Snubber resistance R_s (Ohms)	$1e^5$
3.	Power Electronic device	IGBT/Diodes
4.	On resistance R_{on} (Ω)	$1e^{-3}$
5.	Falling time T_f (Sec)	$1e^{-6}$
6.	Total time T_t (Sec)	$2e^{-6}$

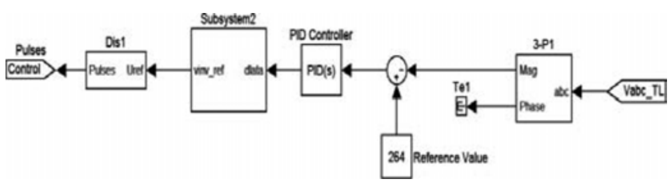

Fig. 9. MATLAB/Simulink model of Inverter firing pulses.

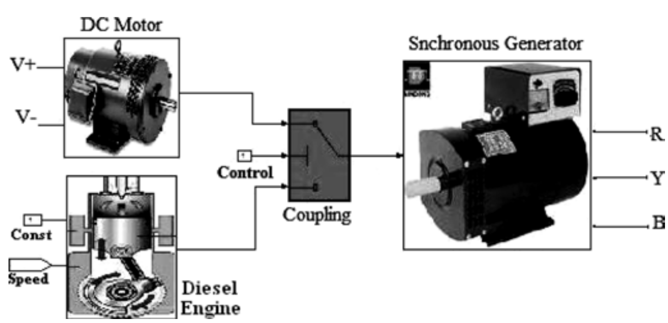

Fig. 10. MATLAB/Simulink model of dc motor/Diesel engine-Synchronous generator set.

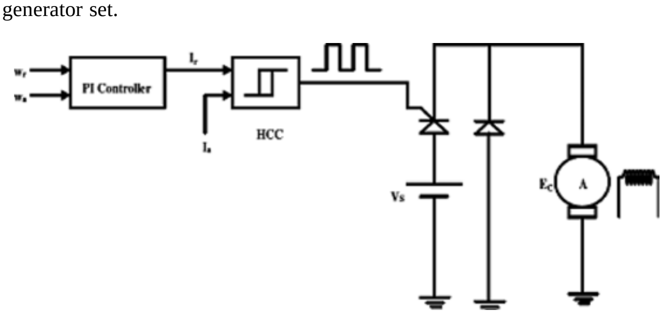

Fig. 11. Speed controller circuit for dc Motor.

speed controller mode. For alternator model, select Simplified Synchronous Machine SI units in Sim power systems/machines from simulink library with the parameters given in Table III.

TABLE III
PARAMETERS FOR ALTERNATOR MODELING

S. No	Parameter	Description
1.	Connection type	3-wire Y
2.	Mechanical Input	Speed (w)
3.	Nominal Power (P_n) in VA	$50e^3$
4.	Line-to-Line Voltage (V_n rms)	440 V
5.	Frequency (F_n) in Hz	50
6.	Internal Resistance R (Ω)	0.0204
7.	Internal Inductance L (Henries)	$0.08104e^{-3}$

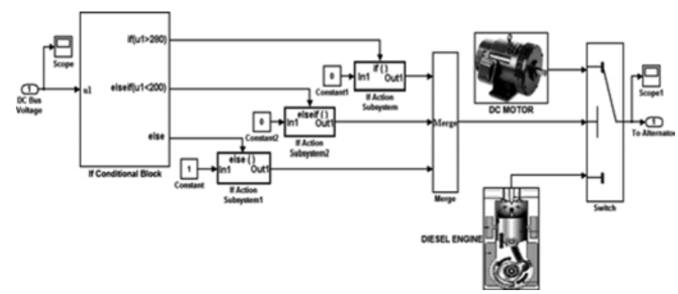

Fig. 12. MATLAB/Simulink model for switching between dc Motor and Diesel engine to drive alternator.

It is very much desired to keep the power quality as high always irrespective of loads or environmental conditions, to interface the system with the utility power grid. This demands the system to have constant voltage, frequency, and output signal in sinusoidal shape, etc., hence, it is always intended to control the frequency. It can be achieved by controlling the speed of the motor, as it is directly proportional to the frequency as per the (4). For the synchronous generator the speed is given by the equation

$$N_S = \frac{120 \times f}{P} \text{ (In rpm)} \tag{4}$$

where:

N_S synchronous speed;

f frequency;

P number of poles.

The PI (Proportional and Integral) controller is used to provide the necessary control action [39]–[41] for the field winding of the motor. It takes two inputs namely, the actual output speed and the reference speed.

To ensure continuous prime mover energy to synchronous generator, the diesel engine set up is coupled as a stand by prime mover. The control logic shown in Fig. 12 checks the condition of available resources and dc bus ratings to know whether the dc bus voltage is enough for dc motor to drive the alternator. In the conditions where dc motor is unable to drive alternator, the control logic isolates dc motor and connects the diesel engine [35] as the prime mover to the alternator.

E. MATLAB/Simulink Model of Retrofitted HPS Design

Fig. 13 shows the model for overall architecture of the proposed retrofitted HPS design. As explained earlier initially all the energy sources are connected to dc bus through local controllers. This dc bus drives the input to MG set. The MG set consists of a dc motor coupled to an alternator that supplies power to the loads. This arrangement will improve the power quality

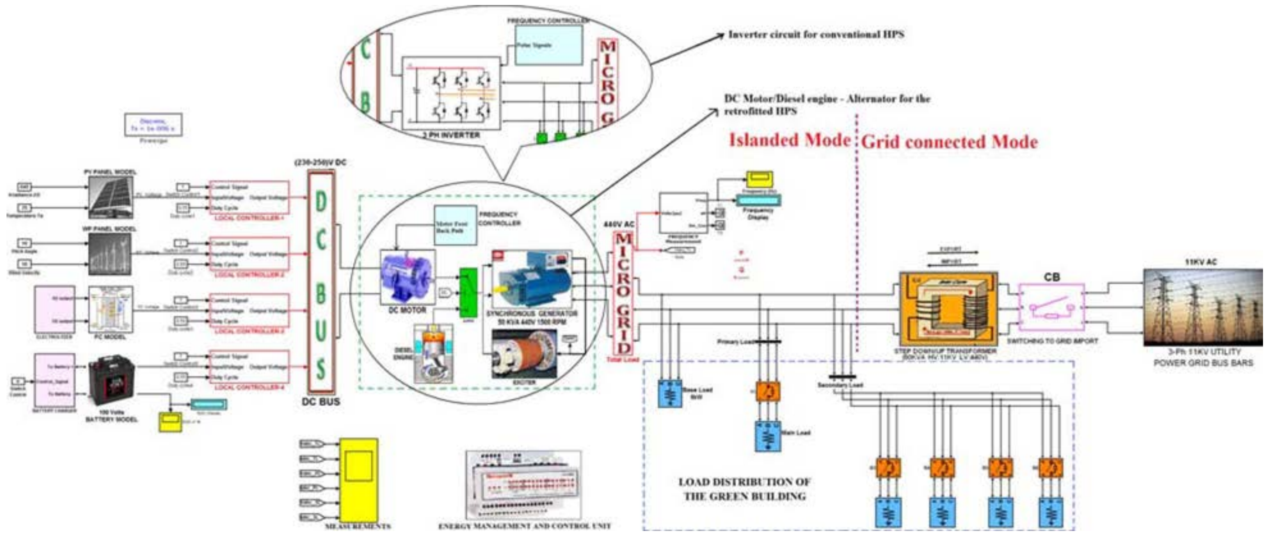

Fig. 13. MATLAB/Simulink model of the proposed retrofitted Hybrid Power System architecture for buildings.

and eliminates the major drawbacks with the conventional HPS architectures. MG set technology is used as a very efficient "line conditioner" providing both voltage stabilization and harmonic rejection. It can also prevent any line to line noise entering into the output because of the shaft or belt connection.

Besides the usage of MG set, the proposal also includes design of EMCU. The typical operation of the EMCU is to control the local controllers and grid synchronizing unit. The grid synchronizing unit consists of a circuit breaker (CB) and step-up/down transformer. The operating conditions of this unit as per the inputs from the EMCU are:

- Isolating mode from grid;
- Grid export/import mode.

As shown in Fig. 13, in the grid interaction mode, CB is activated with the command from EMCU. The EMCU checks the status of power generation, load requirement, and emergency or fault situations and sends corresponding signals to the CB. CB is "ON" for grid importing/exporting modes and "OFF" for islanding (fault/synchronization issues) modes. The transformer operates as 11 KV at High Voltage (HV) side and with 440 V at Low Voltage (LV) side to provide facility of "import from grid" when there is deficit power in the HPS and "export to grid" when there is excess power in the HPS, that's providing two way operation. Fig. 14 shows the EMCU control flow.

V. Energy Management and Control Unit

The Energy Management and Control Unit (EMCU) switch the mode of power supply among all the available resources to meet the instantaneous load demand on the system [13], [26]. The proposed algorithm for EMCU is shown in Fig. 14. It takes the generated power and the load demand as the inputs. And these two are compared against each other to check for different conditions.

If generated power exceeds the load, then excess power will be collected by the electrolyzer of the fuel cell. The Electrolyzers are used to absorb the rapidly fluctuating output power with load. The electrolyzer can produce H_2 gas and is stored in H_2 reservoir tank. This is used as the fuel for fuel cells, which reduces the fuel cost. EMCU monitors the H_2 reservoir tank. If H_2 reservoir tank is full, excess power is used to charge the battery. The storage batteries compensate the load supply when the output power is deficient. Its charging status is also monitored by the EMCU on time. The typical operation of the EMCU can be described as follows.

- EMCU compares P_G and P_L to use available resources optimally with respect to the power demand.
- It checks for the following conditions
  - $P_G \geq P_L$
  - $P_G < P_L$

  According to these conditions, some of the available energy sources will be switched on to meet the demand exactly, while some sources may be in rest.
- In the control flow shown in Fig. 14, the dc bus power ($P_{\mathrm{dc}} = P_G$) is calculated as the sum of the powers of all the available resources. And the load demand P_L is the combined demand of all classes of loads at any instant.
- Initially, PV and WP systems are switched on since there is no input fuel cost for them.
- At this condition the EMCU compares the generated power P_G and the total load at any instant P_L.
- If P_G is more than P_L, that indicates the generation of excess power, this excess power is used to charge the batteries or in the process of hydrogen production in Electrolyzer/Reformer. If the EMCU finds still excess power, it will switch on the grid synchronizing unit in export mode, so that excess power is exported to the grid.
- If P_G is less, that indicates the generation of deficit power, in these cases the fuel cell unit is switched on while the fuel cell and battery charging is off.
- Further, the batteries are also switched on if required depending on load, and if still it is found as deficit, the remaining power demand is supplied by central grid, i.e., the EMCU switches the synchronizing unit to grid import mode.
- This process of switching between the resources continues by depending upon the load demands and environmental conditions.
- In any fault or emergency conditions where there is a scope of loss of synchronism, EMCU opens the grid synchronizing unit to isolate HPS with utility grid.

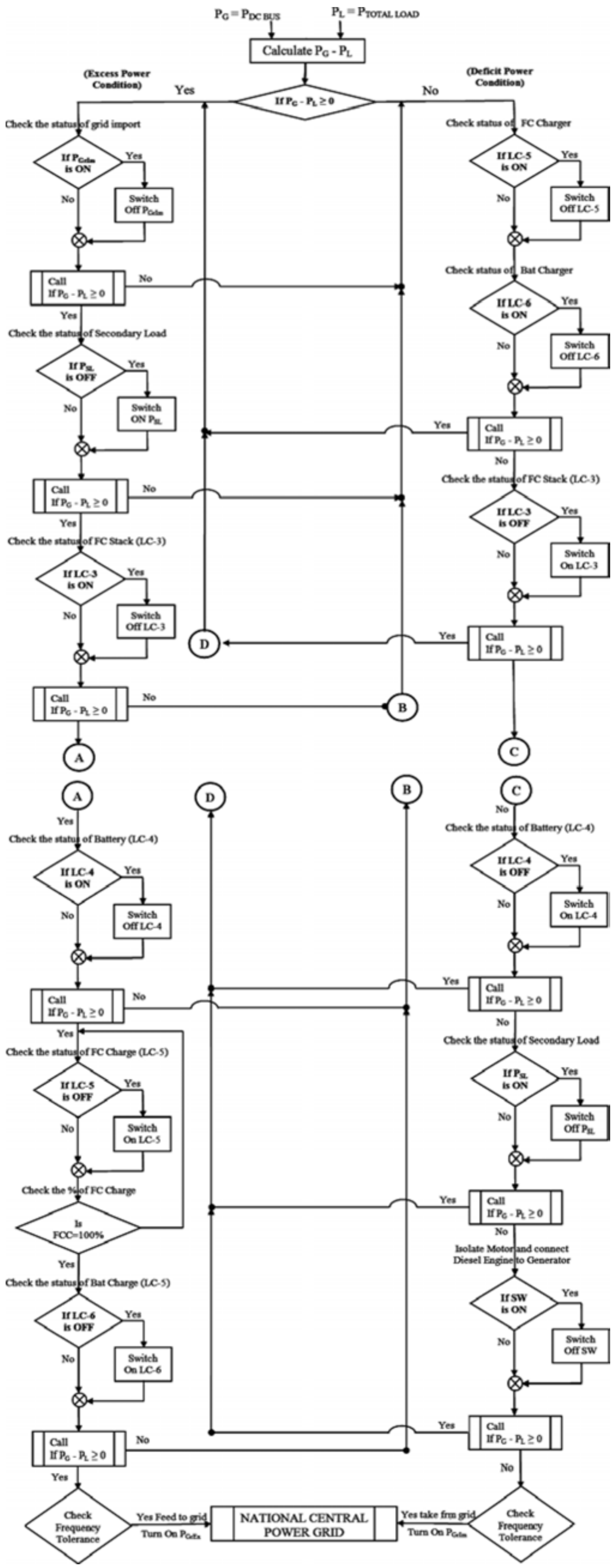

Fig. 14. Proposed Algorithm for EMCU.

- Hence, the usage of this EMCU makes the system more reliable, stable, and economic by reducing effective use of energy.

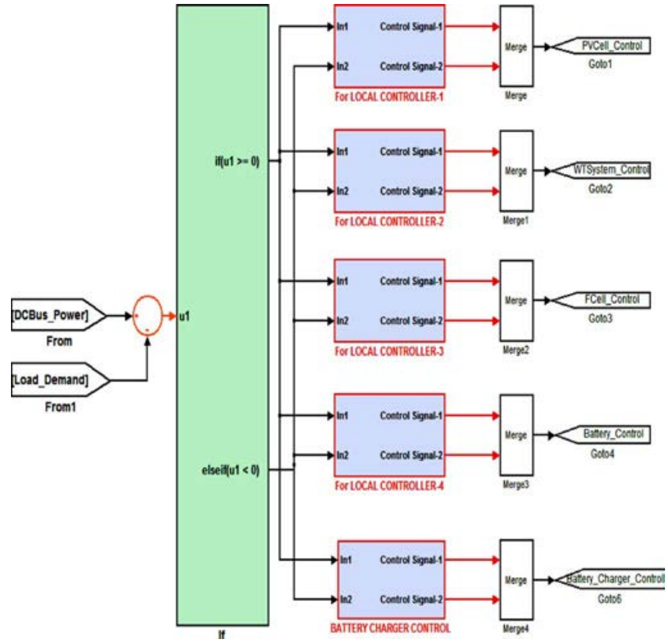

Fig. 15. MATLAB/Simulink model of EMCU.

In the relatively low capacity of the micro-gird (island mode) power systems [17], [18], there are flexible choices for demand side to increase the efficiency of the system operation and economics. Therefore, using demand side management to opportunely control load, would reduce the need of generation capacity and increase the utilization [4] of renewable generation devices and accordingly increase the efficiency of generation investment.

Fig. 15 shows the MATLAB/Simulink model of the EMCU logic for local controller signals. It gives the control signals to the local controllers to switch between the resources depending upon the various dynamic conditions discussed earlier.

The Hybrid Power System is based on the multi-agent theory [12], where the control subsystem is regarded as an agent [19]. Each agent will act as a local controller for that area and connected to the central EMCU to perform the role of data acquisition and communication as shown in Figs. 4 and 13. The agent takes the control signals from the EMCU and manages the operation of the local microgrid, (or) power sources like wind turbine generation, solar photovoltaic, Fuel cell, storage batteries, etc.

VI. Simulation Results and Discussions

As per the objective of this paper, the results obtained are focusing on the following two aspects.

- Power quality improvement
- Energy management and control unit (EMCU) operation

A. Power Quality Issues: Retrofitted HPS (Vs) Prior Art

In little more than ten years, electricity power quality has grown from obscurity to a major issue. Power electronic devices gave birth to numerous new applications, offering unmatched comfort, flexibility and efficiency to the utilities. The technological advancement in electronic field resulted into sophisticated equipments. These equipments are highly sensitive to poor power quality. These require reliable and good quality power free from all quality issues. Hence, electricity power quality is becoming a major issue for the utilities.

The power quality problem is defined as any problem manifested in voltage, current or frequency deviations that result in malfunctioning of building equipment. The power quality problem causes the deterioration of performance of various sensitive electronic and electric equipments in the buildings. Good power quality is characterized as follows.

- The supply voltage should be within guaranteed tolerance of declared value.
- The wave shape should be pure sine wave within allowable limits for distortion.
- The voltage should be balanced in all three phases.
- Supply should be reliable, i.e., continuous availability without interruption.

In order to compare the effectiveness of the proposed retrofitted HPS architecture with the exiting topology, various critical parameters related to power quality are considered and obtained as follows.

1. Total Harmonic Distortion (THD)
2. Energy Conversion Efficiency Calculation (η)
3. Electrical Efficiency $(\eta_{\text{electrical}})$
4. Variation in the Magnitude of Supply voltage
5. Voltage Dip (Sag) and Swells
6. Voltage Imbalance/Unbalance
7. Frequency Variations

1) Total Harmonic Distortion (THD): The first and foremost power quality parameter is the Total Harmonic Distortion (THD). The THD of a periodic signal is a measurement of the harmonic distortion present, and is defined as the ratio of the sum of the squared individual harmonic amplitudes to the fundamental frequency (or) the root mean square (RMS) value of the total harmonics of the signal, divided by the RMS value of its fundamental signal. The signal can be a measured voltage or current.

For example, for currents, the THD is defined as

$$\text{Total Harmonic Distortion (THD)} = \frac{I_H}{I_F} \tag{5}$$

where $I_H = \sqrt{I_2^2 + I_3^2 + \cdots + I_n^2}$, and

I_H RMS value of the Hth harmonic;

I_F RMS value of the fundamental current.

Fig. 16 shows the MATLAB/Simulink model for calculating THD [2]. The main reason for harmonic distortion is a nonlinear load. So, in the analysis of this THD, a nonlinear load (power electronics device load) is connected to the system at time 0.5 sec as shown in Figs. 17 and 18, and FFT analysis of the current wave for three cycles is done with a maximum frequency of 1000 Hz.

From Figs. 17 and 18, the THD values obtained for an inverter based HPS (added 3-Ph "L-filter" of $L = 2$ mH in series to the inverter output) and proposed MG set based HPS are obtained as 4.87% and 4.61% respectively. Hence the harmonic distortion value is reduced with the proposed HPS architecture.

2) Energy Conversion Efficiency (η): The output of any electrical machine is always less than the input, because some of the energy is lost in the form of heat during each stage of energy conversion. Therefore, this energy loss and the energy conversion efficiency for the inverter based and proposed MG set based HPS is calculated as follows.

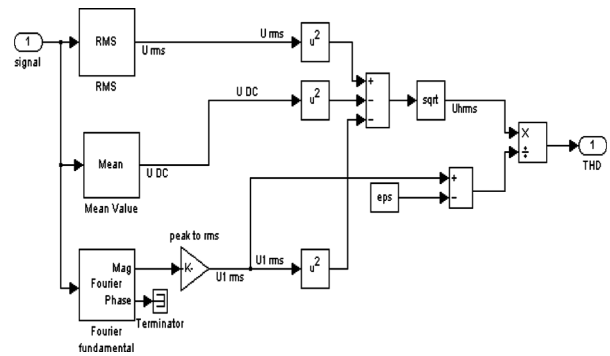

Fig. 16. Matlab/Simulink Modeling of THD block.

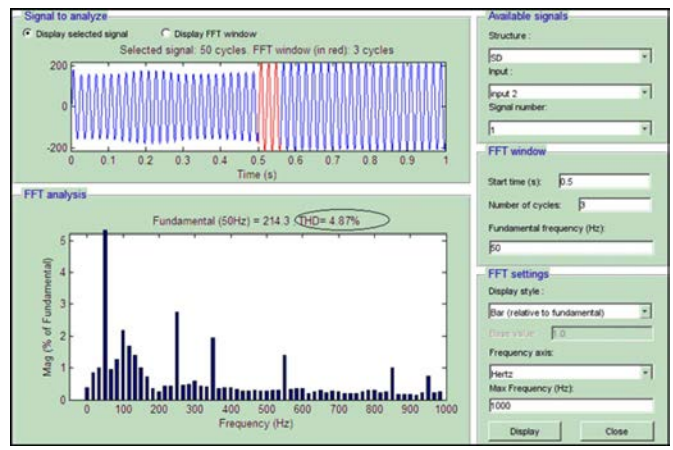

Fig. 17. THD analysis for generic HPS architecture.

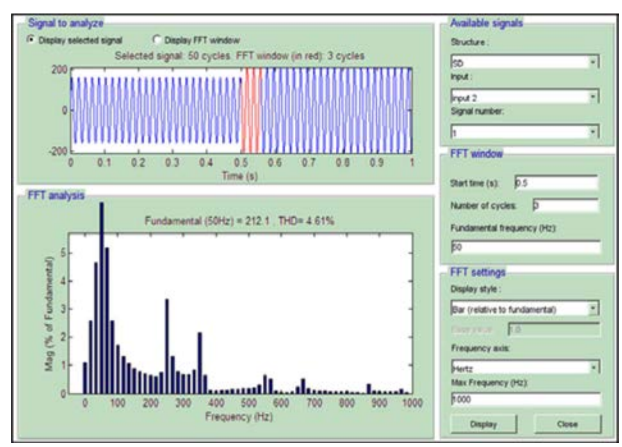

Fig. 18. THD analysis for retrofitted HPS architecture.

For DC Motor and Generator Set: The losses in the MG set can be classified broadly into the following types.

- Electrical loss (Energy losses in the form of $I^2 \times R \times t$)
- Mechanical loss (Losses in the shaft and mechanical transmission)

Energy conversion efficiency of a dc motor is defined as the ratio of electrical equivalent of mechanical power developed and total electrical power input, and is denoted with $\eta_{\text{dc Motor}}$

$$\therefore \eta_{dcMotor} = \frac{E_b I_a}{VI} \tag{6}$$

Energy conversion efficiency of alternator is defined as a ratio of the total electrical power output in stator and electrical equivalent of mechanical power input, and is denoted with $\eta_{\text{Alternator}}$.

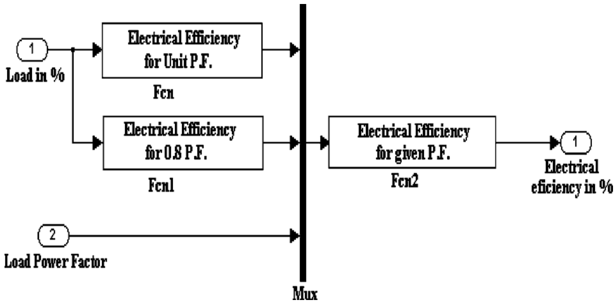

Fig. 19. Matlab/Simulink Model for electrical efficiency.

The overall Energy conversion efficiency of the combination, i.e., MG set is as follows.

$$\therefore \eta_{Overall} = \eta_{dcMotor} \times \eta_{Alternator} \tag{7}$$

(Mechanical losses are not considered in the simulation, since, MATLAB models/blocks are ideals. This loss is approximated for a 100 kW rating of machine (both motor/generator) with allowable error. The losses are calculated at 90% of full load).

The total losses in the $\mathrm{dc\ motor} = 5282\ \mathrm{Watts}$ $[\mathrm{Electrical\ loss} = 4282\ \mathrm{watts},\ \mathrm{Mechanical\ loss} = 1000\ \mathrm{watts}$ (assumed)]

$$\eta_{dcMotor} = \frac{90\ \mathrm{kW}}{90\ \mathrm{kW} + 5.282\ \mathrm{kW}} = 0.9445$$

$\therefore$ Motor Efficiency $(\eta_{dcMotor}) = 94.45\%$

Total losses in the $\mathrm{Alternator} = 2618\ \mathrm{Watts}$ $[\mathrm{Electrical\ loss} = 1798\ \mathrm{watts},\ \mathrm{Constant\ loss} = 820\ \mathrm{watts}$ (assumed)]

$$\eta_{Alternator} = \frac{90\ \mathrm{kW}}{90\ \mathrm{kW} + 2.618\ \mathrm{kW}} = 0.9717$$

$\therefore$ Alternator Efficiency $(\eta_{alternator}) = 97.17\%$

Overall energy conversion efficiency of the MG set,

$$\therefore \eta_{Overall} = 0.9445 \times 0.9717 \times 100 = 91.78\%$$

Inverter Model: As this is a static device with no rotating part, no mechanical loss appears in such devices. But however a certain amount of loss occurs due to the high frequency switching of the power electronic devices. This type of losses are called switching loss. Total losses in this model found to be are very less, with an efficiency of around 97%, (It is calculated simply by dividing the output power of the inverter to the input power of the inverter at the same load, i.e., at 90% of full load).

$$\therefore \eta_{Overall} = 97.0\%$$

3) Electrical Efficiency $(\eta_{electrical})$*:* The electrical efficiency is a measure of utilizing generated power by the loads. It is the ratio of the load demand to the generating capacity of the plant. The modeling equations [42] to find electrical efficiency are the fourth order polynomials and given for unity power factor, 0.8 power factor, and for a given load with (8), (9), and (10) respectively. Fig. 19 shows the Matlab/Simulink model for finding electrical efficiency. Figs. 20 and 21 show the electrical efficiency in both generic and proposed HPS system for different loads.

For a load (L) of UPF

$$\eta_{\mathrm{el1}} = (-6.953e^{-9} \times L^4) + (2.932e^{-7} \times L^3) + (-9.858e^{-4} \times L^2) + (0.201 \times L) + 81.372 \tag{8}$$

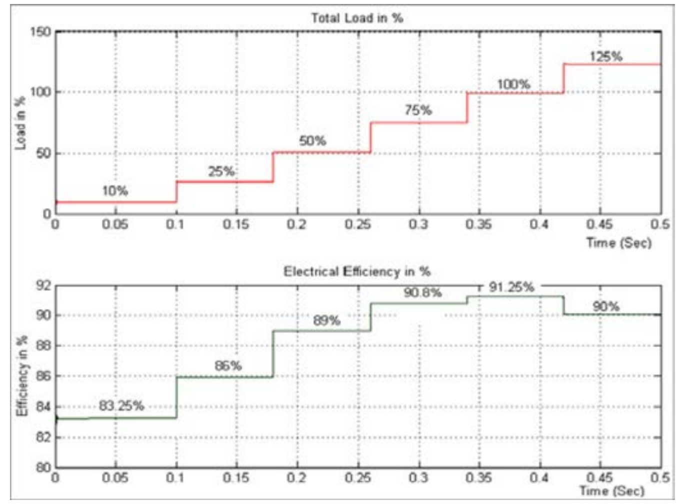

Fig. 20. Electrical Efficiency at different loads for retrofitted HPS architecture.

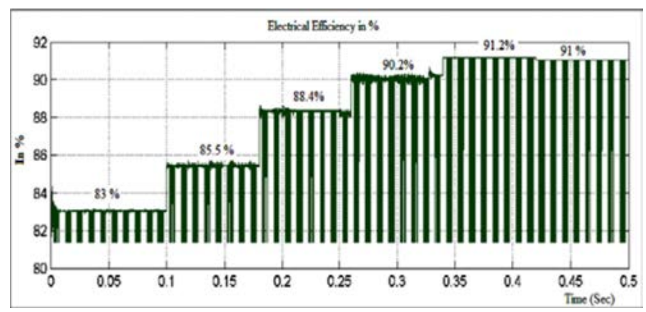

Fig. 21. Electrical Efficiency at different loads for Generic HPS architecture.

For a load (L) of 0.8 PF

$$\eta_{\mathrm{el2}} = (1.540e^{-7} \times L^4) + (-4.424e^{-5} \times L^3) + (2.996e^{-3} \times L^2) + (0.034^L) + 81.652 \tag{9}$$

Hence, for the given loads, the electrical efficiency is

$$\eta_{\mathrm{el}} = \eta_{\mathrm{el2}} + \left(\frac{\eta_{el1} - \eta_{el2}}{0.2} \times (pf - 0.8)\right) \tag{10}$$

4) Variation in the Magnitude of Supply Voltage: Long-duration variations in supply voltages encompass root-mean-square (rms) deviations at power frequencies for longer than 1 min. Long-duration variations can be either over-voltages or under-voltages. An over-voltage is an increase in the RMS ac voltage more than 110% at the power frequency for duration longer than 1 min. An under-voltage is a decrease in the RMS ac voltage to less than 90% at the power frequency for duration longer than 1 min.

These are caused by the load variation in the system and switching operations. Overvoltage is caused by load switching (e.g., switching off a large load or energizing a capacitor bank). A load switching ON or a capacitor bank switching OFF can cause under-voltage. These changes are mainly due to reactive power mismatch. These might also happen when the microgrid is switched from grid connected mode to stand alone mode (mismatch in reactive power).

These variations can be measured in the simulation by initiating the following.

- A large inductive load is switched ON/OFF
- A large capacitive load is switched ON/OFF
- Grid—connected and disconnected modes.

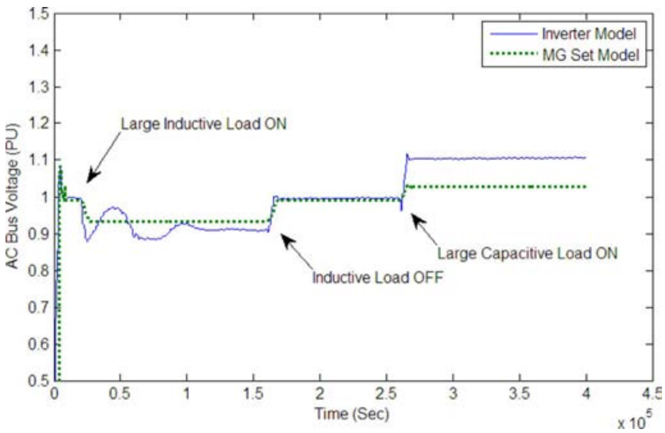

Fig. 22. Variation in the supply voltage for load variations.

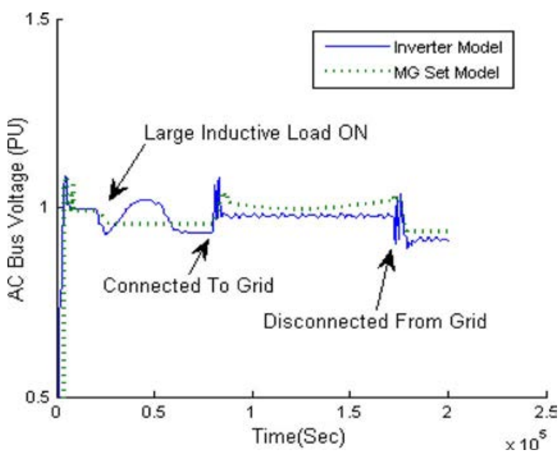

Fig. 23. Variation in the supply voltage in sudden grid connected and isolated modes.

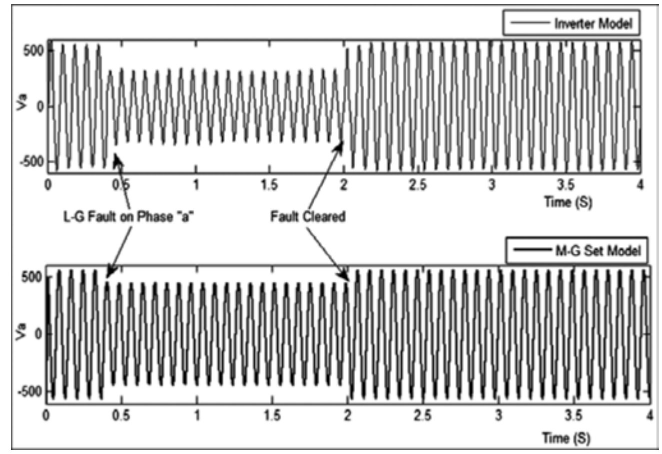

Fig. 24. Comparison of Voltage Sag of faulted phase for both generic and retrofitted HPS systems.

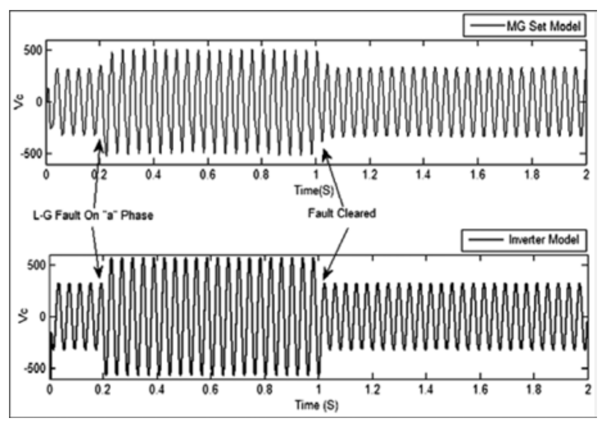

Fig. 25. Comparison of Voltage Swell of un-faulted phase for both generic and retrofitted HPS systems.

Figs. 22 and 23 gives the variation in the magnitude of the supply voltage for these conditions. From these results, it can be clearly observed that these variations are smooth and low even for very long duration in the case of proposed HPS.

5) Voltage Dip (Sag) and Swells: Voltage dip (Sag) is a decrease between 0.1 and 0.9 Pu in rms voltage at the power frequency for durations from 0.5 cycles to 1 min. A swell is defined as an increase to between 1.1 and 1.8 Pu in rms voltage or current at the power frequency for the durations from 0.5 cycles to 1 min.

Sag is associated with the system fault at distribution network or near a large industrial load. This can also happen during starting of a large motor. Switching off a large load or energizing a large capacitor bank can also cause swells. The sag and swell in the system is evaluated by initiating an L-G fault on the system near the load end.

For the voltage sag analysis, the fault is allowed to persist for 1.5 seconds on the line "a" and then it is cleared. Fig. 24 illustrates the "sag" or "dip" in the faulted phase voltage for both, inverter based and proposed MG set based system. And it is observed that the voltage sag is 42% in the Inverter based conventional HPS and 21.6% in the proposed MG set based HPS, which improves the signal quality compared to the earlier case.

The swell is observed on the unfaulted phase. For the voltage swell analysis, the fault is allowed to persist for 0.8 seconds on the line "a" and then it is cleared. Fig. 25 illustrates the formation of "swell" in the unfaulted phase voltage for both, inverter based and proposed MG set based system. And it is observed that the voltage swell is 40% in the Inverter based conventional HPS and 28% in the proposed MG set based HPS, which improves the signal quality compared to the earlier case.

6) Voltage Imbalance/Unbalance: Voltage imbalance (also called voltage unbalance) is defined as the maximum deviation from the average of the three-phase voltages, divided by the average of the three-phase voltages, expressed in percentage. (Or) The ratio of the negative or zero sequence components to the positive sequence component is usually expressed as a percentage.

The primary source of voltage unbalance is single-phase loads on a three-phase circuit. Voltage unbalance can also be the result of blown fuses in one phase of a three-phase capacitor bank.

It can be measured by measuring the $+\mathrm{ve}$ sequence, $-\mathrm{ve}$ sequence, and zero sequence voltage.

A single phase load is switched "ON" on the three phase line at a particular time and the $-\mathrm{ve}$ sequence voltage is observed. The percentage imbalance s calculated by using (11).

$$\%\mathrm{Imbalance} = \frac{-VeSequence\_Voltage}{+VeSequence\_Voltage} \times 100 \qquad (11)$$

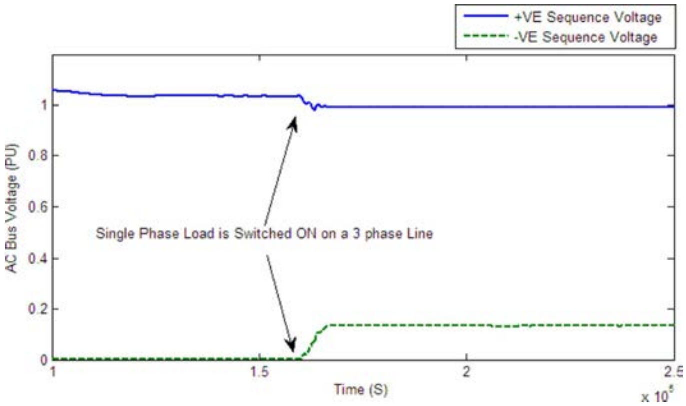

Fig. 26. Positive and Negative Sequence voltages of Inverter based generic HPS.

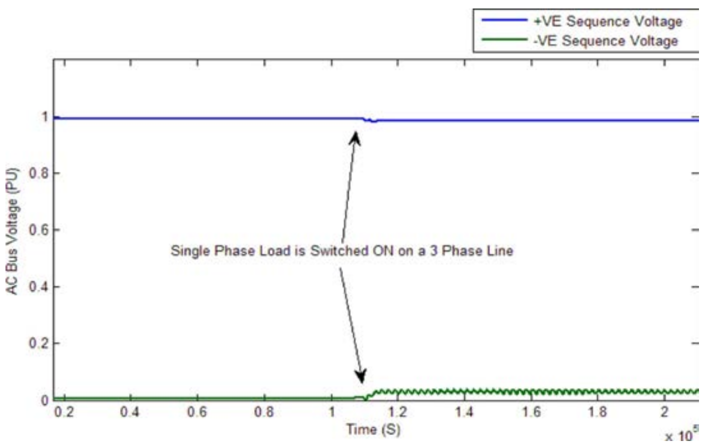

Fig. 27. Positive and Negative Sequence voltages of MG set based retrofitted HPS.

And for the both HPS architectures, the positive and negative sequence voltages are shown in Figs. 26 and 27. The imbalance in the voltage is calculated as follows:

$$\%\,\text{Imbalance for Inverter set} = \frac{0.133}{1}100\% = 13.3\%$$

$$\%\,\text{Imbalance for MG set} = \frac{0.03}{1} \times 100 = 3\%$$

7) Frequency Variation: As per the standards of the Indian utility power grid frequency should be 50 Hz with an allowable tolerance of $\pm 3\%$, i.e., 48.5 Hz to 51.5 Hz [43]. Figs. 28 and 29, represents the frequency in both the architectures controlled for variations in building load taken in the paper.

Table IV gives the cumulative comparison of Inverter based generic HPS system and MG set based proposed retrofitted HPS in various power quality parameters discussed above.

8) Energy Management and Control in Retrofitted HPS: The EMCU manages the energy flow between all available resources and the load requirement. EMCU is much needed in the renewable energy based systems because these are quite environmental dependent, which is fairly unpredictable. So, to ensure continuous supply to loads, EMCU plays a very critical role.

Figs. 30–32 show the input variations to the HPS like variations in wind power, solar power, and load demands. Based on these conditions at each instant EMCU takes total power generated (P_G) and total load demand (P_L) as inputs and manages, controls the HPS system.

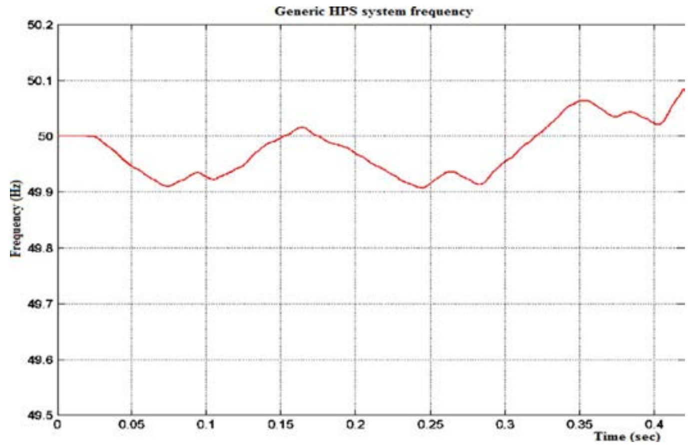

Fig. 28. Overall system frequency for generic HPS.

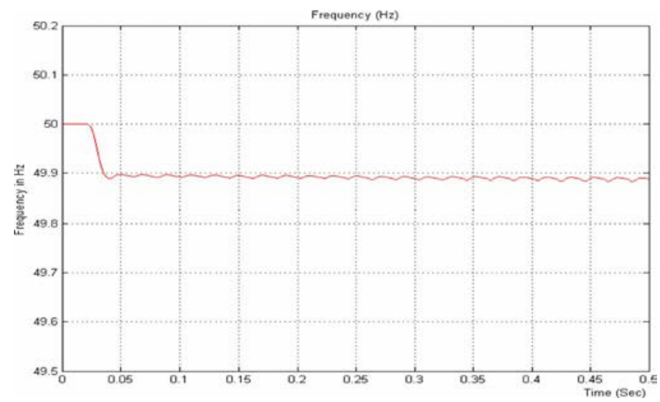

Fig. 29. Overall system frequency for retrofitted HPS.

TABLE IV
THE PERFORMANCE METRICS

S. No	Parameter	Inverter based generic HPS	MG set based retrofitted HPS
1.	Total Harmonic Distortion (THD)	4.87 % (Figure.17)	4.61 % (Figure.18)
2.	Energy Conversion efficiency	97.0 % (Section VI-A-2)	91.78 % (Section VI-A-2)
3.	Electrical Efficiency (At different % of full load)	25% load= 85.5% 50% load= 88.4% 75% load= 90.2% 100% load= 91.2% 120% load=91.0% (Figure.21)	25% load= 86.0% 50% load= 89.0% 75% load= 90.8% 100% load= 91.3% 120% load= 90.0% (Figure.20)
4.	Variation in the voltage for the reactive load variations	Noisy and High compared to proposed HPS (Figure.22)	Smooth and Low compared to generic HPS (Figure.22)
5.	Variation in the voltage for grid exchanges	Noisy (Figure.23)	Smooth (Figure.23)
6.	Voltage Sag	42 % (Figure.24)	21.6 % (Figure.24)
7.	Voltage Swell	40 % (Figure.25)	28 % (Figure.25)
8.	Voltage Imbalance	13.3 % (Figure.26)	3 % (Figure.27)
9.	Frequency (Max Deviation)	± 0.4% (Figure.28)	± 0.22% (Figure.29)

Fig. 33 shows the dc Bus ratings namely power, voltage, and current. The dc bus is maintained at voltage (230–250) Volts.

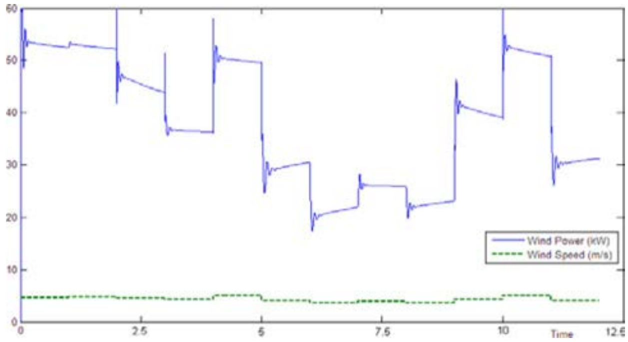

Fig. 30. Variation in the wind power with respect to the variation in wind velocity.

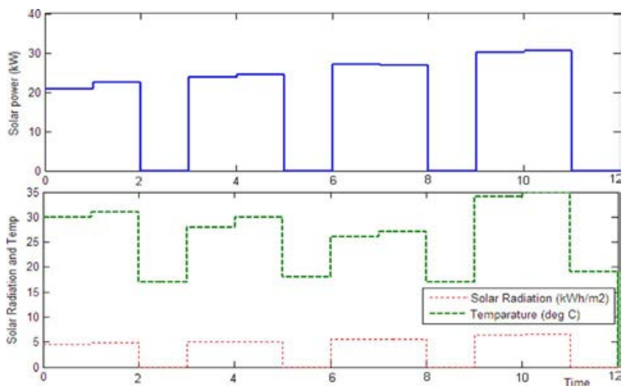

Fig. 31. Variation in the solar power with respect to the variation in solar radiation and temperature.

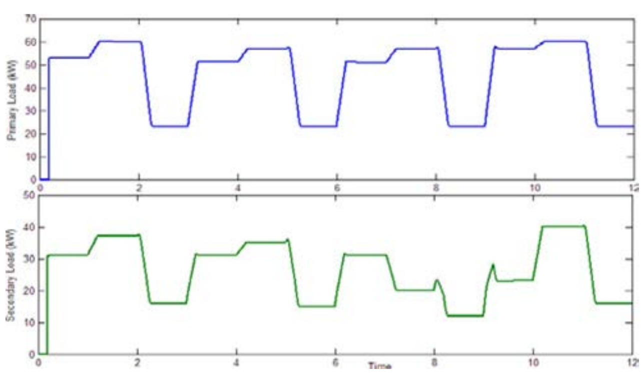

Fig. 32. Load variations in primary and secondary loads.

Since, these are the dc values, and hence the power is available as the multiplication of voltage and current as in the (12).

$$Power = Voltage \times Current = V \times I \tag{12}$$

Fig. 34 shows the line voltage (peak) of the microgrid and is related as shown in the (13)–(16).

$$V_{Line} = \sqrt{3} \times V_{Phase} \tag{13}$$

$$\therefore\ V_{Line} = \sqrt{3} \times (230 - 250)$$

$$\cong (400 - 440)\ \text{Volts} \tag{14}$$

$$V_{Line(peak)} = \sqrt{2} \times V_{Line} \tag{15}$$

$$\therefore V_{Line(peak)} = \sqrt{2} \times 440 = 622\ \text{Volts} \tag{16}$$

The EMCU always checks the emergency or fault conditions along with the total load demand and power generated. Based on all these conditions it operates the grid-synchronizing unit in three modes (Export/Import/Isolate). This facilitates the optimum use of energy sources, which increases the reliability of the system to meet the demand, while sustaining the load always.

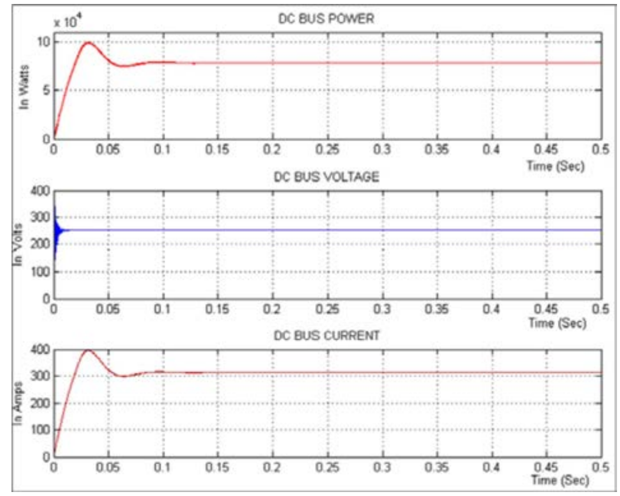

Fig. 33. DC Bus Power, Voltage, and Current.

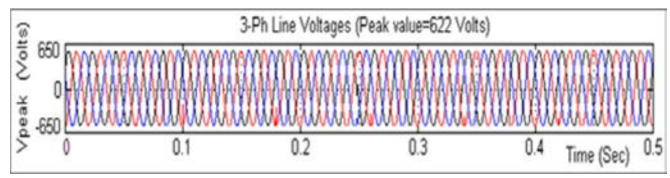

Fig. 34. 3-Ph line voltages (peak) in retrofitted HPS.

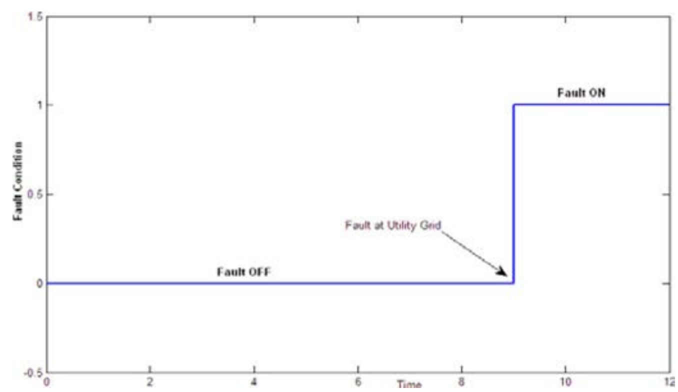

Fig. 35. Applying fault condition on the microgrid.

Fig. 35 shows the occurrence of a fault on the system and Figs. 36 and 37 show the EMCU Control signal to the grid-synchronizing unit and behavior of grid communication with respect to load demand and power generated respectively.

VII. Conclusions

Conventional architectures of the renewable energy based Hybrid Power Systems are majorly associated with power quality issues as discussed in Section II. This is the primary concern which leads for the novelty in this paper. The paper is focused on the design of renewable energy based HPS with power quality improvement and energy management features.

The methodology introduced is the use of a dc Motor-Synchronous generator set instead of an inverter, to interface energy sources with building loads/grid as shown in Fig. 13. To have an optimum usage of the available resources, an EMCU is designed. It works based on the total power generated and the instantaneous load demand.

From the results obtained in Section VI (A&B), the following conclusions have been made.

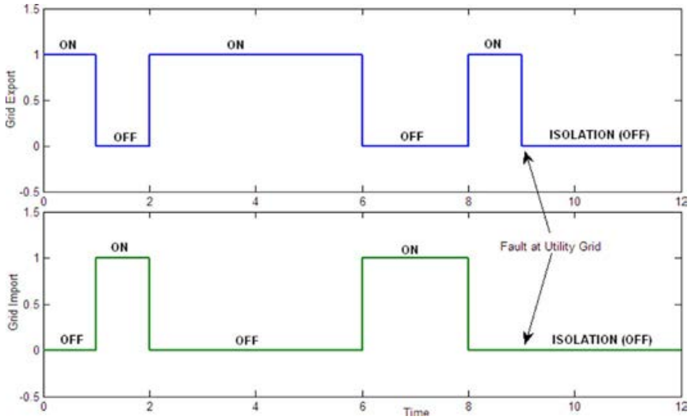

Fig. 36. EMCU Control signals to grid synchronizing unit for grid import/export/isolate.

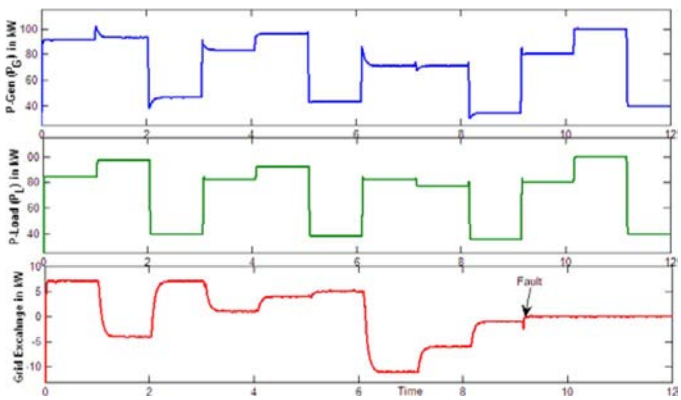

Fig. 37. Grid exchange (import/export/isolate).

- The voltage sag/swell levels for faults are less in the proposed architecture compared to generic HPS.
- As per IEEE Std 929–2000 [44], total harmonic current distortion shall be less than 5% of the fundamental frequency current. This is achieved by the proposed design. THD for the proposed is 4.61%, and that is for the conventional HPS is 4.87%.
- The voltage variations with respect to the grid exchanges or reactive load changes are less and smooth in the proposed retrofitted structure.
- Voltage imbalances and frequency variations are less in the retrofitted design, which indicates preserving the shape of sinusoid.
- The HPS system can effectively communicate with the utility power grid to export/import the excess/deficit power respectively.
- The EMCU can also isolate the system from utility power grid under loss of synchronism.

These points indicate that the retrofitted system helps in improving power quality in buildings and facilitates the application of HPS for grid-connected mode effectively. The results show that the proposed EMCU is capable of managing the switching between available resources with respect to load fluctuations and environmental conditions.

Hence, this retrofitted system allows the facilities to export, import, generate, and use power without violating any regulations and tolerate the rapid changes in load and environment. This ensures continuous, stable, and reliable supply to loads by providing optimum utilization of energy resources for economic and quality power generation.

VIII. Limitations of the Proposed HPS Design

Besides its numerous advantages, the proposed layout may have the following limitations.

- The efficiency of the proposed system is low compared to the conventional inverter based systems as evaluated in the Section VI-A2
- The cost of unit generation might be a concern when the HPS is intended to supply power to a small to medium range power rating buildings in real time scenarios, since a lot of cost has to incur towards machine running, maintenance, and repairing.

In spite of these minor deviations from the conventional designs, the novelty can produce green and sustainable energy where the world is looking into in the current trend.

References

[1] B. Delfino and F. Fornari, "Modeling and control of an integrated fuel cell-wind turbine system," in *Proc. 2003 IEEE Bologna Power Tech Conf.*, pp. 23–26.
[2] Math Works Central [Online]. Available: http://www.mathworks.com/
[3] A. Rowe and X. Li, "Mathematical modeling of proton exchange membrane fuel cells," *J. Power Sources*, pp. 82–96, 2001.
[4] S. M. Shaahid and M. A. Elhadidy, "Technical assessment of grid independent photovoltaic-diesel-battery power systems for commercial loads in desert environments," *Renewable Sustainable Energy Reviews*, vol. 11, pp. 1794–1810, 2007.
[5] O. Ulleberg, "Stand-alone power systems for the future: optimal design, operation and control of solar-hydrogen energy systems," Ph.D. dissertation, Norwegian Univ. Sci. Technol., Trondheim, 1997.
[6] K. Sapru, N. T. Stetson, and S. R. Ovshinsky, "Development of a small scale hydrogen production storage system for hydrogen applications," in *Proc. 1997 Intersociety Conf.*, vol. 3, pp. 1947–1952.
[7] M. J. Khan and M. T. Iqbal, "Dynamic modeling and simulation of a small wind-fuel cell hybrid energy system," *Renewable Energy*, vol. 30, pp. 421–439, 2005.
[8] D. B. Nelson *et al.*, "Unit sizing and cost analysis of stand- alone hybrid wind/PV/fuel cell power generation systems," *Renewable Energy*, vol. 31, pp. 1641–1656, Aug. 2006.
[9] B. C. Kuo, *Automatic Control Systems*, 7th ed. New York: Prentice-Hall, 1995.
[10] H.-C. Chen, J.-C. Qiu, and C.-H. Liu, "Dynamic modeling and simulation of renewable energy based hybrid power systems," in *Proc. DRPT*, Apr. 2008, pp. 2803–2809.
[11] T. T. Chan, *Transient Analysis of Integrated Solar/Diesel Hybrid Power System Using MATLAB Simulink*. Melbourne, Australia: School of Electrical Engineering, Victoria Univ., 2008.
[12] L. Guangming, C. Yuanrui, and L. Tao, "The realization of control system in the energy management of wind/solar hybrid system," in *Proc. Int. Conf. Power Electron. Syst. Appl.*, 2009.
[13] C. Wang and M. H. Nehrir, "Power management of a standalone wind/photovoltaic/fuel cell energy system," *IEEE Trans. Energy Convers.*, vol. 23, no. 3, pp. 957–967, Sep. 2008.
[14] Y. J. Reddy and Y. V. P. Kumar, "Power quality improvement, energy management using PLCs in hybrid power systems," in *Proc. Conf. Electr. Syst. Renewables*, 2011, pp. 44–51.
[15] A. Mohd, E. Ortjohann, W. Sinsukthavorn, M. Lingemann, N. Hamsic, D. Morton , and , "Supervisory control and energy management of an inverter-based modular smart grid," in *Proc. 2009 IEEE/PES Power Syst. Conf. Expo.*, pp. 1–6.
[16] O. Omari, E. Ortjohann, A. Mohd, and D. Morton , "An online control strategy for DC coupled hybrid power systems," in *Proc. 2007 IEEE Power Eng. Soc. Gen. Meet.*, pp. 1–8.
[17] J. C. V. Quintero and J. M. Guerrero, *Decentralized Control Management Applied to Power DGs in Microgrid-Renewable Energy Integration Towards the Smart Grid*. Saarbrucken, Germany: Lambert Academic, 2010.
[18] R. Majumder, *Microgrid: Stability Analysis and Control-Modeling, Stability Analysis and Control of Microgrids for Improved Power Sharing and Power Flow Management*. Dusseldorf, Germany: VDM Verlag Dr. Muller, 2010.
[19] C. Rehtanz, *Autonomous Systems and Intelligent Agents in Power System Control and Operation*. New York: Springer-Verlag, 2010.

[20] R. Sankarayogi, *Software Tools for Real-Time Simulation and Control-Hardware in the Loop, Supervisory Options*. Dusseldorf, Germany: VDM Verlag Dr. Muller, 2010.

[21] B. S. Borowy and Z. M. Salameh, “Dynamic response of a stand-alone wind energy conversion system with battery energy storage to a wind gust,” *IEEE Trans. Energy Convers.*, vol. 12, no. 1, pp. 73–78, Mar. 1997.

[22] M. Arifujjaman, M. T. Iqbal, J. E. Quaicoe, and M. J. Khan, “Modeling and control of a small wind turbine,” in *Proc. Can. Conf. Electr. Comput. Eng.*, 2005, pp. 778–781.

[23] K. De Brabandere, K. Vanthournout, J. Driesen, G. Deconinck, and R. Belmans, “Control of microgrids,” in *Proc. 2007 IEEE Power Eng. Soc. Gen. Meet.*, pp. 1–7.

[24] M. Ibrahim, Decentralized Hybrid Renewable Energy Systems M.Sc. thesis, Univ. Kassel. Kassel, Germany, 2002.

[25] R. Saiju, O. Omari, and E. Ortjohann, “A simulation model for expandable hybrid power systems,” in *Proc. Kasseler Symp.*, Kassel, Germany, 2002.

[26] U.S. Environmental Protection Agency, Green Building Home, 2009 [Online]. Available: http://www.epa.gov/greenbuilding/

[27] WBDG Sustainable Committee 2009 [Online]. Available: http://www.wbdg.org/designsustainable.php

[28] S. Pushkar, R. Becker, and A. Katz, “A methodology for design of environmentally optimal buildings by variable grouping,” *Building Environ.*, vol. 40, pp. 1126–1139, 2005.

[29] T. Senjyu, T. Nakaji, K. Uezato, and T. Funabashi, “A hybrid power system using alternative energy facilities in isolated island,” *IEEE Trans. Energy Convers.*, vol. 20, no. 2, pp. 406–414, Jun. 2005.

[30] R. Chedid and S. Rahman, “Unit sizing and control of hybrid wind-solar power systems,” *IEEE Trans. Energy Convers.*, vol. 12, no. 1, pp. 79–85, 1997.

[31] E. S. Gavanidou and A. G. Bakirtzis, “Design of a stand-alone system with renewable energy using Trade-Off methods,” *IEEE Trans. Energy Convers.*, vol. 7, no. 1, pp. 42–48, 1992.

[32] R. R. Kumar, I. Abouzahr, and K. Ashenayi, “A knowledge based approach to the design of integrated renewable energy systems,” *IEEE Trans. Energy Convers.*, vol. 7, no. 4, pp. 648–655, 1992.

[33] Y. J. Reddy, A. Ramsesh, K. P. Raju, and Y. V. P. Kumar, “A novel approach for modeling and simulation of hybrid power systems using PLCs and SCADA for hardware in the loop test,” in *Proc. IET Int. Conf. Sustainable Energy Intell. Syst.*, Tamil Nadu, India, Jul. 2011, vol. 2, pp. 545–553.

[34] Y. J. Reddy, K. P. Raju, and Y. V. P. Kumar, “Real time and high fidelity simulation of hybrid power system dynamics,” in *Proc. IEEE Int. Conf. Recent Adv. Intell. Comput. Syst.*, Sep. 2011.

[35] Y. J. Reddy, K. P. Raju, and Y. V. P. Kumar, “Use of DC Motor-generator set for power quality improvement in a renewable energy based hybrid power system,” *Int. J. Recent Trends Eng. Technol.*, vol. 05, no. 02, pp. 182–185, Mar. 2011.

[36] J. Singh, R. Mittal, and D. K. Jain, “Improved performance of diesel driven permanent magnet synchronous generator using battery energy storage system,” in *Proc. IEEE Electr. Power Energy Conf.*, 2009.

[37] K. E. Yeager and J. R. Wills, “Modeling of emergency diesel generators in an 800 megawatt nuclear power plant,” *IEEE Trans. Energy Convers.*, vol. 8, no. 3, pp. 433–441, Sep. 1993.

[38] B. S. Borowy and Z. M. Salameh, “Dynamic response of a stand-alone wind energy conversion system with battery energy storage to a wind gust,” *IEEE Trans. Energy Convers.*, vol. 12, no. 1, pp. 73–78, Mar. 1997.

[39] S. Ayasun and G. L. Karbeyaz, “DC motor speed control methods using MATLAB/Simulink,” *Comput. Appl. Eng. Educ.*, vol. 15, pp. 347–354, 2007.

[40] “Practice 3, DC Motor Control ,” in *Workshop MATLAB/Simulink Drives Power Electron.*, 2009 [Online]. Available: http://www.mathworks.com

[41] B. Singh and S. Prakash, “Intelligent PI controller for speed control of D.C. Motor,” *Int. J. Electron. Eng. Res.*, vol. 2, pp. 87–100, 2010.

[42] A. Agarwal, R. Wies, and R. Johnson, *Hybrid Electric Power Systems-Modeling, Optimization, and Control*. Dusseldorf, Germany: VDM Verlag Dr. Muller, 2011.

[43] “Central Electricity Regulatory Commission,” in *Grid Security—Need for Tightening of Frequency Band & Other Measures*. New Delhi, India: CERC, 2011.

[44] *IEEE Recommended Practice for Utility Interface of Photovoltaic (PV) Systems*, IEEE Std. 929–2000, 2000.

Y Jaganmohan Reddy received the B.Tech. degree in the area of electronics and instrumentation engineering from Kakatiya University, in 1997, the M.Sc. degree in BITS, Pilani, in 2004. He is currently working toward the Ph.D. degree in the field of hybrid power systems and smart grids in Jawaharlal Nehru Technological University Kakinada, India.

Currently, he is working as Senior Systems Engineer in Honeywell Technology Solutions Lab, Hyderabad, India. He has 15 years' experience in the field of industrial automation and control as a Maintenance Engineer, Project Engineer, Test Engineer, and Manager. He has published 17 research papers and 1 international monograph on the concepts of power quality, energy management and real time control, and hardware simulation for hybrid power systems in various national and international conferences/journals.

Y V Pavan Kumar received the B.Tech. degree in electrical and electronics engineering and from Jawaharlal Nehru Technological University Hyderabad, India, in 2007 and the M.Tech. degree in instrumentation and control systems from Jawaharlal Nehru Technological University Kakinada, India, in 2011.

He has two years of teaching experience in electrical and electronics engineering and one year in industrial automation and control systems. Currently he is working as an Engineer in the Engineering Test Services of Aerospace Business Unit, Honeywell Technology Solutions Lab, Hyderabad. He has published 17 research papers in national/international journals/conferences and 1 international monograph in the area of renewable energy. His research area includes power systems, classical and modern control systems, and artificial intelligence.

K. Padma Raju received the B.Tech. degree from Nagarjuna University, India, in 1989, the M.Tech. degree from National Institute of Technology Warangal, India, in 1992, and the Ph.D. degree from Andhra University, India in 2005.

He received a Postdoctoral Fellowship at Hoseo University, South Korea, in 2007. He has worked as a Digital Signal Processing Software Engineer in Signion Systems pvt. Ltd, Hyderabad, India, before joining Jawaharlal Nehru Technological University Kakinada, India. He has 20 years of teaching experience and is Professor of ECE, JNTUK, India. He is currently working as Director, IIIP&T, Jawaharlal Nehru Technological University Kakinada. He worked as Professor at Hoseo University, South Korea during 2006–2007. He has published 30 research papers in National/International Journals/Conferences and guiding 10 research students in the area of Antennas, EMI/EMC and Communications.

Dr. Raju is Fellow of IETE and IE and Life Member of ISTE and SEMCE.

Anil Kumar Ramsesh received the Diploma degree in EE and the B.E. degree in ECE from Bangalore University, India, in 1987 and 1995, respectively, and the M.Sc. degree (Engg) and the Ph.D. degree in solar cell instrumentation from IISc, Bangalore, in 2000 and 2005, respectively.

He is now working as a Fellow Engineer in Honeywell Technology Solutions (P) Ltd, Bangalore. Prior to Honeywell he was with ISRO from 1987 to 2004 and was involved in design of high power switching amplifiers for electro-dynamic vibrators, instruments for cryogenics, instrumentation for solar power systems. He has around 25 disclosures, 14 patents filed, and 4 patents granted to date and has 12 papers in international journals. He is also a Member in Board of Studies and Visiting faculty, School of Electronics, Vellore Institute of Technology, Vellore.